LETTERS

Energetic neutral atoms as the explanation for the high-velocity hydrogen around HD 209458b

M. Holmström[1], A. Ekenbäck[1], F. Selsis[2,3], T. Penz[4], H. Lammer[5] & P. Wurz[6]

Absorption in the stellar Lyman-α (Lyα) line observed during the transit of the extrasolar planet HD 209458b in front of its host star reveals high-velocity atomic hydrogen at great distances from the planet[1,2]. This has been interpreted as hydrogen atoms escaping from the planet's exosphere[1,3], possibly undergoing hydrodynamic blow-off[4], and being accelerated by stellar radiation pressure. Energetic neutral atoms around Solar System planets have been observed to form from charge exchange between solar wind protons and neutral hydrogen from the planetary exospheres[5–7], however, and this process also should occur around extrasolar planets. Here we show that the measured transit-associated Lyα absorption can be explained by the interaction between the exosphere of HD 209458b and the stellar wind, and that radiation pressure alone cannot explain the observations. As the stellar wind protons are the source of the observed energetic neutral atoms, this provides a way of probing stellar wind conditions, and our model suggests a slow and hot stellar wind near HD 209458b at the time of the observations.

Energetic neutral atoms (ENAs) are produced wherever energetic ions meet a neutral atmosphere, and solar wind ENAs have been observed at every planet in the Solar System where ENA instrumentation has been available—for Earth[5], Mars[6] and Venus[7].

By energetic we mean that the ions have a much greater velocity than the thermal velocities of the exospheric neutrals. During the charge exchange process, an electron is transferred from the neutral to the ion, resulting in a neutral atom and an ionized neutral. Because of the large relative velocities of the ions and the exospheric neutrals, the momenta of the individual atoms are preserved to a good approximation. Thus, the produced ENAs will have the same velocity distribution as the source population of ions.

When first observed (also by their Lyα signature[8,9]), the extended hydrogen coronae of Mars and Venus were assumed to constitute the uppermost layers of an escaping exosphere. The observed densities were used to infer exospheric scale heights and temperatures, which proved to be extremely high compared with theoretical predictions (up to 700 K). *In situ* spacecraft observations[10] later found exospheric temperatures of ~210 and ~270 K. The discrepancy was eventually explained by photochemically produced energetic particles, and by ENAs, produced by charge exchange between energetic solar wind protons and the planetary exosphere. Although this mechanism is well known in the Solar System, it has not been considered as a possible origin of the atomic hydrogen corona revealed by Hubble Space Telescope observations of HD 209458b.

HD 209458b is a Jupiter-type gas giant with a mass of $\sim 0.65 M_{\rm Jup}$ and a size of $\sim 1.32 R_{\rm Jup}$ that orbits at ~0.045 AU (ref. 11) around its host star HD 209458, which is a solar-like G-type star with an age of about 4 Gyr. The activity of the star can be estimated from its X-ray luminosity measured by the XMM-Newton space observatory, and is comparable to that of the present Sun during a moderately quiet phase[12]. Because of its Sun-like stellar type and average activity, it is reasonable to use the energy environment observed at the Sun as inputs for our model.

For a first estimate of the ENA production near HD 209458b, we assume that the charge exchange takes place in an undisturbed stellar wind that is flowing radially away from the star. At 0.045 AU from HD 209458, the stellar wind is most likely subsonic[13] and does not produce a planetary bow shock. Simulations indicate a subsolar magnetopause distance of about four planetary radii if the planet is magnetized[14]. If the planet is not magnetized, we would expect the undisturbed stellar wind to get even closer to the planet. Here we model the ENA production by a particle model that includes stellar wind protons and atomic hydrogen. Charge exchange between stellar wind protons and exospheric hydrogen atoms takes place outside a conic obstacle that represents the magnetosphere of the planet (Supplementary Fig. 1). The resulting exospheric cloud, along with the produced ENAs, covers a region larger than the stellar disk, as seen from Earth (Fig. 1). The cloud is shaped like a comet tail owing to the stellar radiation pressure, curved by the Coriolis force, as predicted[15] and seen in earlier numerical simulations[1,3]. There is a population of atoms with high velocity—these are the stellar wind protons that have charge-exchanged, becoming ENAs. In the velocity spectrum along the x axis (the planet–star line), the ENAs are clearly visible as a distribution that is separate from the main exospheric hydrogen component, because of the different bulk velocities and temperatures (Fig. 2).

Now we estimate how the ENA cloud would affect the observed Lyα absorption spectrum of HD 209458b[1]. The line profile was observed outside and during transit, and the difference between the two profiles corresponds to the attenuation by hydrogen atoms (Fig. 3).

There are several features of the transit spectrum that any proposed source of the observed hydrogen atoms needs to account for. First, there are hydrogen atoms with velocities of up to $-130\,{\rm km\,s^{-1}}$ (away from the star). Second, there is a fairly uniform absorption over the whole velocity range -130 to $-45\,{\rm km\,s^{-1}}$. Third, there is absorption in the velocity range between 30 and $105\,{\rm km\,s^{-1}}$ (towards the star).

The current explanation of the observation is that hydrogen atoms in the exosphere are undergoing hydrodynamic escape, and are further accelerated by the stellar radiation pressure[1,4]. But there are difficulties in explaining the observations by this process, as can be seen by examining the three features listed above.

First, a large radiation pressure on the hydrogen atoms is needed to accelerate them to a velocity of $130\,{\rm km\,s^{-1}}$ before they are

[1]Swedish Institute of Space Physics, PO Box 812, SE-98128 Kiruna, Sweden. [2]Laboratoire d'Astrophysique de Bordeaux (CNRS, Université Bordeaux 1), BP 89, F-33270 Floirac, France. [3]Centre de Recherche Astrophysique de Lyon (CNRS, Université de Lyon, Ecole Normale Supérieure de Lyon), 46 Allée d'Italie, F-69007 Lyon, France. [4]INAF—Osservatorio Astronomico di Palermo, Piazza del Parlamento 1, I-90134 Palermo, Italy. [5]Space Research Institute, Austrian Academy of Sciences, Schmiedlstrasse 6, A-8042 Graz, Austria. [6]Physikalisches Institut, University of Bern, Sidlerstrasse 5, CH-3012 Bern, Switzerland.

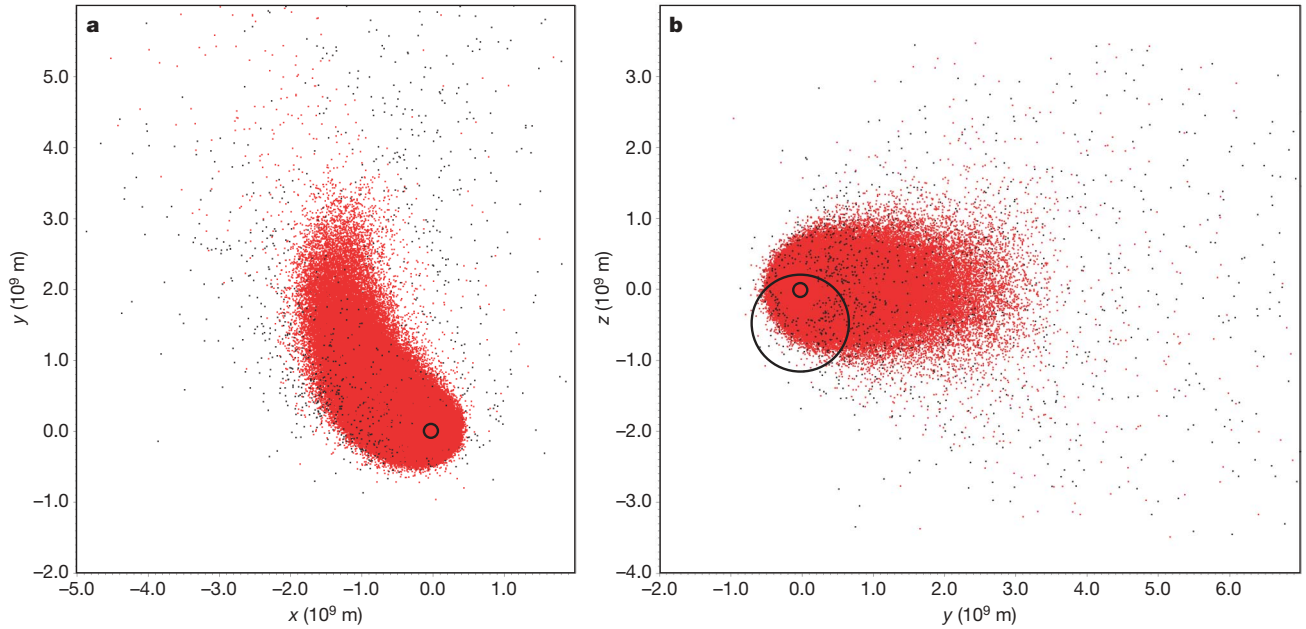

Figure 1 | The hydrogen cloud around the planet. **a**, Shown from above, perpendicular to the planet's orbital plane; **b**, as seen from Earth, along the direction of the *x* axis. Each point corresponds to a hydrogen meta particle. The colour of the points shows the velocity of the particles along the *x* axis. Particles with velocity magnitude smaller than 50 km s^{-1} are red, and those with higher velocity are black. The small circles show the planet size. The large circle in **b** shows the star's position at mid-transit. During transit the star moves from left to right in **b**. At the outer boundaries of the simulation domain, stellar wind protons are injected with a number density of 2×10^3 cm^{-3}, velocity 50 km s^{-1} and temperature10^6 K. The planet's interaction with the stellar wind is modelled by removing all stellar wind protons inside a conic obstacle at a substellar distance of about $4.2R_p$ (where the radius of the planet $R_p = 9.4 \times 10^7$ m). Hydrogen atoms are launched from an inner boundary (a sphere of radius $2.1R_p$) assuming a number density of 10^8 cm^{-3} and a temperature of 7,000 K, consistent with atmospheric models[18]. The trajectory of each proton and hydrogen atom is followed in time. The forces on a hydrogen atom are the gravity of the planet, the Coriolis force due to the rotating coordinate system, and radiation pressure. After each time step a hydrogen atom can undergo photoionization, elastic collision with another hydrogen atom or charge exchange with a proton. The photoionization time assumed is 4 h which is a scaled Earth value. The radiation pressure corresponds to a photon–hydrogen collision rate of 0.35 s^{-1} and is chosen to improve the model fit. It is lower than a scaled Earth value of 0.6–1.6 s^{-1} over a solar cycle. The coordinate system used is centred at the planet with its *x* axis towards the star, and the *y* axis opposite to the planet's velocity. Further details of the simulations can be found in the Supplementary Information.

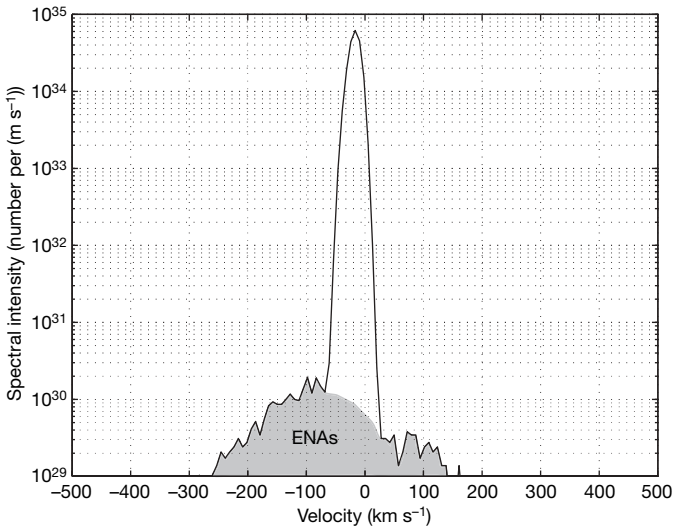

Figure 2 | Velocities of the hydrogen atoms. The modelled *x* axis (planet–star) velocity spectrum of hydrogen atoms in front of the star at the moment of mid-transit, not including atoms in front or behind the planet. The part of the distribution that is due to ENAs is shaded. Varying the stellar wind temperature and velocity in the model confirms that the width of this part of the distribution is proportional to the temperature of the stellar wind, with a larger width for larger temperatures, and the centre of the distribution follows the stellar wind velocity. The unshaded part of the spectrum is due to the exospheric hydrogen atoms.

photoionized. The acceleration must occur before they move out from the region in front of the star, owing to the orbital motion of the planet. The second feature is difficult to explain. If hydrogen atoms were driven to speeds of up to 130 km s^{-1}, we would expect the velocity spectrum to have an exponential decay for higher velocities, because photoionization gives the hydrogen atoms a finite lifetime (four hours on average). This drop-off for high velocities is independent of the details of the model, for example the values of radiation pressure and photoionization lifetime used. This would lead to a decay in the absorption spectrum, inconsistent with the observed fairly uniform absorption over the whole velocity range -130 to -45 km s^{-1}. Finally, an exosphere driven by radiation pressure cannot explain hydrogen atoms moving towards the star with speeds between 30 and 105 km s^{-1}. However, this feature is not completely certain, and more observations may be needed to clarify whether an absorption is present in the red part of the line (towards the star)[1].

Our model shows that the three observed features can be explained by ENAs. If we turn off the ENA production in the model, none of these features are explained. When we compare the modelled Lyα profile with the observed ones, we find that the modelled spectrum leads to attenuation over the whole velocity range from -130 to -45 km s^{-1}, as observed. The model also shows some absorption in the red part of the velocity spectrum, that is, hydrogen atoms moving at high velocities towards the star, because for this stellar wind (50 km s^{-1} and 10^6 K), some part of the proton velocity distribution will have positive velocities along the *x* axis, resulting in an ENA flux towards the star. This slow and hot stellar wind is not unrealistic at such small orbital distances[13].

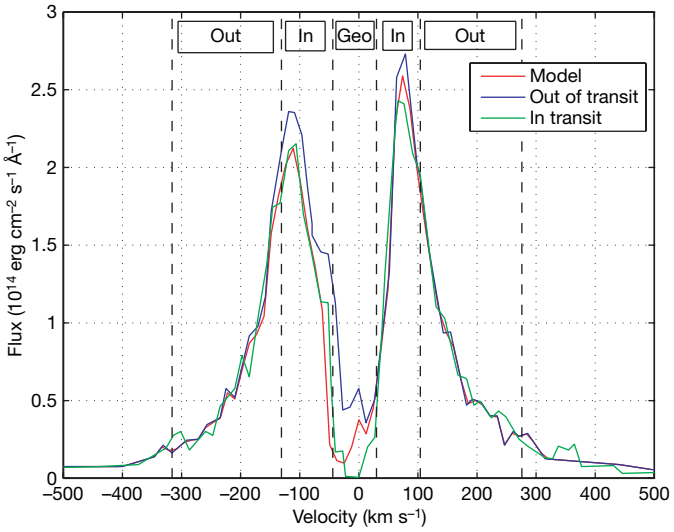

Figure 3 | Comparison of modelled with observed Lyα profiles. Blue, the observed profile before transit. Green, the observed profile during transit. Red, the modelled profile, constructed by applying the attenuations computed from the simulations to the observed profile before transit. The abscissa is the hydrogen velocity along the *x* axis (away from Earth, towards the star). The regions where there is a significant difference between the profiles are denoted 'In' and 'Geo', the latter being the region of geocoronal emission at low velocities that should be excluded. The modelled profile is computed at the instant of mid-transit. The details of computing the Lyα attenuation from the hydrogen cloud are given in the Supplementary Information. The modelled Lyα absorption shown here is for a stellar wind velocity of 50 km s^{-1} and a temperature of 10^6 K. The fit is worse for stellar wind velocities of 0 or 100 km s^{-1}, or stellar wind temperatures of 2×10^6 K or 0.5×10^6 K (see Supplementary Information).

If ENAs from charge exchange are responsible for the observed attenuation, we have, on the one hand, much less information on the main exospheric component than suggested by previous explanations. Because what we observe are mainly ENAs, a range of exospheric conditions and atmospheric loss rates can be consistent with the observation. The observation only constrains atmospheric escape insofar as the exosphere has to be extended enough to reach the stellar wind outside the planet's magnetopause. The atmospheric escape through ENA production is small. For the model parameters used here, the loss is 7×10^5 kg s^{-1}, more than an order of magnitude smaller than the estimated thermal loss of about 10^7 kg s^{-1} for similar exospheric conditions[16–18].

On the other hand, we gain information on the underlying plasma flows, and if this is the undisturbed stellar wind, we have a way of observing stellar wind properties such as temperature and velocity around other stars, at the location of extrasolar planets. By varying the stellar wind temperature, the stellar wind velocity and the radiation pressure in the model, we find a best fit of the modelled Lyα absorption to the observation for a stellar wind velocity of 50 km s^{-1}, and a temperature of 10^6 K (Fig. 3).

Although, for HD 209458b, the available Lyα data are affected by large uncertainties, more accurate observations would improve the derived stellar wind estimates. Also, the depletion of the stellar wind proton flow by charge exchange will change the character of the interaction between planet and stellar wind. Present models of the stellar wind interaction with HD 209458b have not taken this process into account[14]. More observations of the Lyα absorption by HD 209458b, and its variation over time, could be used to confirm the origin of the extended hot hydrogen cloud. There should be more variability on short timescales for absorption by ENAs than for other explanations, such as hydrodynamic escape, because stellar wind parameters can change significantly on a timescale of hours, as seen near Earth.

Received 19 September; accepted 11 December 2007.

1. Vidal-Madjar, A. *et al.* An extended upper atmosphere around the extrasolar planet HD209458b. *Nature* **422,** 143–146 (2003).
2. Ben-Jaffel, L. Exoplanet HD 209458b: Inflated hydrogen atmosphere but no sign of evaporation. *Astrophys. J.* **671,** L61–L64 (2007).
3. Vidal-Madjar, A. & Lecavelier des Etangs, A. in *Extrasolar Planets: Today and Tomorrow*, ASP Conf. Ser. 321 (eds Beaulieu, J.-P., Lecavelier des Etangs, A. & Terquem, C.) 152–159 (Astronomical Society of the Pacific, 2004).
4. Vidal-Madjar, A. *et al.* Detection of oxygen and carbon in the hydrodynamically escaping atmosphere of the extrasolar planet HD 209458b. *Astrophys. J.* **604,** L69–L72 (2004).
5. Collier, M. R. *et al.* Observations of neutral atoms from the solar wind. *J. Geophys. Res.* **106,** 24893–24906 (2001).
6. Futaana, Y. *et al.* First ENA observations at Mars: Subsolar ENA jet. *Icarus* **182,** 413–423 (2006).
7. Galli, A. *et al.* First observation of energetic neutral atoms in the Venus environment. *Planet. Space Sci.* advance online publication doi:10.1016/j.pss.2007.12.011 (1 January 2008).
8. Barth, C. A. Interpretation of the Mariner 5 Lyman alpha measurements. *J. Atmos. Sci.* **25,** 564–567 (1968).
9. Barth, C. A. *et al.* Marine 6: Ultraviolet spectrum of mars upper atmosphere. *Science* **165,** 1004–1005 (1969).
10. Lichtenegger, H. I. M. *et al.* Effects of low energetic neutral atoms on martian and venusian dayside exospheric temperature estimations. *Space Sci. Rev.* **126,** 469–501 (2006).
11. Knutson, H., Charbonneau, D., Noyes, R. W., Brown, T. M. & Gilliland, R. L. Using stellar limb-darkening to refine the properties of HD 209458b. *Astrophys. J.* **655,** 564–575 (2007).
12. Penz, T., Micela, G. & Lammer, H. Influence of the evolving stellar X-ray luminosity distribution on exoplanetary mass loss. *Astron. Astrophys.* **477,** 309–314 (2008).
13. Preusse, S., Kopp, A., Büchner, J. & Motschmann, U. Stellar wind regimes of close-in extrasolar planets. *Astron. Astrophys.* **434,** 1191–1200 (2005).
14. Preusse, S., Kopp, A., Büchner, J. & Motschmann, U. MHD simulation scenarios of the stellar wind interaction with Hot Jupiter magnetospheres. *Planet. Space Sci.* **55,** 589–597 (2007).
15. Schneider, J., Rauer, H., Lasota, J. P., Bonazzola, S. & Chassefiere, E. *Brown Dwarfs and Extrasolar Planets* ASP Conf. Series 134 (eds Rebolo, R., Martin, E. L. & Zapatero Osorio, M. R.) 241–244 (Astronomical Society of the Pacific, Provo, Utah, 1998).
16. Yelle, R. V. Aeronomy of extra-solar giant planets at small orbital distances. *Icarus* **170,** 167–179 (2004).
17. Yelle, R. V. Aeronomy of extra-solar giant planets at small orbital distances: Corrigendum *Icarus* **183,** 508 (2006).
18. García Muñoz, A. Physical and chemical aeronomy of HD 209458b. *Planet. Space Sci.* **55,** 1426–1455 (2007).

Supplementary Information is linked to the online version of the paper at www.nature.com/nature.

Acknowledgements This study was carried out within the framework of the International Space Science Institute team "Evolution of Exoplanet Atmospheres and their Characterization". T.P. is supported by the Marie Curie Fellowship project ISHERPA and the host institution INAF—Osservatorio Astronomico di Palermo. H.L. thanks ASA for funding the CoRoT project. The research used the resources of HPC2N, Umeå University, and LUNARC, Lund University, Sweden. The software was in part developed by the DOE-supported ASC/Alliance Center for Astrophysical Thermonuclear Flashes at the University of Chicago.

Author Contributions A.E. wrote an initial version of the simulation code. F.S. helped in modelling the observation. T.P. provided knowledge on the atmospheres of extrasolar planets. H.L. suggested that the HST observation could be due to ENAs. P.W. contributed expertise in ENA processes

Author Information Reprints and permissions information is available at www.nature.com/reprints. Correspondence and requests for materials should be addressed to M.H. (matsh@irf.se).